

# Optimal projection to improve parametric importance sampling in high dimension

Maxime El Masri · Jérôme Morio · Florian Simatos

**Abstract** In this paper we propose a dimension-reduction strategy in order to improve the performance of importance sampling in high dimension. The idea is to estimate variance terms in a small number of suitably chosen directions. We first prove that the optimal directions, i.e., the ones that minimize the Kullback–Leibler divergence with the optimal auxiliary density, are the eigenvectors associated to extreme (small or large) eigenvalues of the optimal covariance matrix. We then perform extensive numerical experiments that show that as dimension increases, these directions give estimations which are very close to optimal. Moreover, we show that the estimation remains accurate even when a simple empirical estimator of the covariance matrix is used to estimate these directions. These theoretical and numerical results open the way for different generalizations, in particular the incorporation of such ideas in adaptive importance sampling schemes.

**Keywords** Importance sampling · High dimension · Gaussian covariance matrix · Kullback–Leibler divergence · Projection

## 1 Introduction

Importance Sampling (IS) is a widely considered stochastic method to estimate integrals of the form  $E = \int \phi f$  with a black-box function  $\phi$  and a probability density function (pdf)  $f$ . It rests upon the choice of an auxiliary density which, when suitably chosen, can significantly improve the situation compared to the naive Monte Carlo (MC) method (Owen and Zhou (2000); Agapiou et al. (2017)). The theoretical optimal IS density also called zero-variance density is defined by  $\phi f/E$  when  $\phi$  is a positive function. This density is not available in practice as it involves the unknown integral  $E$ , but a classical strategy consists in searching an optimal approximation in a parametric family of densities. By minimising a “distance” with the optimal IS density, such as the Kullback–Leibler divergence, one can find optimal parameters in this family to get an efficient sampling pdf. Adaptive Importance Sampling (AIS) algorithms, such as the Mixture Population Monte Carlo method (Cappé et al. (2008)), the

---

M.El Masri  
ONERA/DTIS, Université de Toulouse, F-31055 Toulouse, France  
ISAE-SUPAERO and Université de Toulouse, Toulouse, France  
E-mail: max.elmasri@outlook.fr

J.Morio  
ONERA/DTIS, Université de Toulouse, F-31055 Toulouse, France  
E-mail: jerome.morio@onera.fr

F.Simatos  
ISAE-SUPAERO and Université de Toulouse, Toulouse, France  
E-mail: florian.simatos@isae.fr

Adaptive Multiple Importance Sampling method (Cornuet et al. (2012)), or the Cross Entropy method (Rubinstein and Kroese (2011)), estimate the optimal parameters adaptively by updating intermediate parameters (Bugallo et al. (2017)).

An intense research activity has made these techniques work very well, but only for moderate dimensions. In high dimension, most of these techniques actually fail to give efficient parameters for two reasons. The first one is the so-called weight degeneracy problem, which is that in high dimension, the weights appearing in the IS densities (which are self-normalized likelihood ratios) degenerate. More precisely, the largest weight takes all the mass, while all other weights are negligible so that the final estimation essentially uses only one sample, see for instance Bengtsson et al. (2008) for a theoretical analysis in the related context of particle filtering. But even without likelihood ratios, such techniques may fail if they need to estimate high-dimensional parameters such as covariance matrices, whose size increases quadratically in the dimension (Ledoit and Wolf (2004); Ashurbekova et al. (2020)). The conditions under which importance sampling is applicable in high dimensions are notably investigated in a reliability context in Au and Beck (2003): it is remarked that the optimal covariance matrix should not deviate significantly from the identity matrix. The authors of El-Laham et al. (2019) tackle the weight degeneracy problem by applying a recursive shrinkage of the covariance matrix, which is constructed iteratively with a weighted sum of the sample covariance estimator and a biased, but more stable, estimator. Concerning the second problem of having to estimate high-dimensional parameters, the idea was recently put forth to reduce the effective dimension by only estimating these parameters (in particular the covariance matrix) in suitable directions (Uribe et al. (2020); El Masri et al. (2020)). In this paper we seek to delve deeper into this idea. The main contribution of the present paper is to identify the optimal directions in the fundamental case when the parametric family is Gaussian, and perform numerical simulations in order to understand how they behave in practice.

The paper is organised as follows: in Section 2 we recall the foundations of IS. In Section 3, we state our main theoretical result and we compare it with the current state-of-the-art. We also position our paper, i.e., we justify the numerical framework that we have adopted. Section 4 presents the proof of our theoretical result, while Section 5 contains numerical results that assess the efficiency of the directions that we propose. We conclude in Section 6 with a summary and research perspectives.

## 2 Importance Sampling

We consider the problem of estimating the following integral:

$$E = \mathbb{E}_f(\phi(\mathbf{X})) = \int \phi(\mathbf{x})f(\mathbf{x})d\mathbf{x}$$

where  $\mathbf{X}$  is a random vector in  $\mathbb{R}^n$  with probability density function (pdf)  $f$ , and  $\phi : \mathbb{R}^n \rightarrow \mathbb{R}_+$  is a real-valued, non-negative function. The function  $\phi$  is considered as a black-box function which is potentially expensive to evaluate, which means the number of calls to  $\phi$  should be limited. We also assume that  $f$  is the standard normal density: this is not a theoretical limitation as we can in principle always come back to this case by transforming the vector  $\mathbf{X}$  with isoprobabilistic transformations (see for instance Liu and Der Kiureghian (1986); Hohenbichler and Rackwitz (1981)).

Importance Sampling (IS) is a widely considered approach to reduce the variance of the classical Monte Carlo estimator of  $E$ . The idea of IS is to generate a random sample  $\mathbf{X}_1, \dots, \mathbf{X}_N$  from an auxiliary density  $g$ , instead of  $f$ , and to compute the following estimator:

$$\hat{E}_N = \frac{1}{N} \sum_{i=1}^N \phi(\mathbf{X}_i)L(\mathbf{X}_i) \quad (1)$$

with  $L = f/g$  the likelihood ratio, or importance weight, and the density  $g$ , called importance sampling density, is such that  $g(\mathbf{x}) = 0$  implies  $\phi(\mathbf{x})f(\mathbf{x}) = 0$  for every  $\mathbf{x}$  (which makes the product  $\phi L$  well-defined). This estimator is consistent and unbiased but its accuracy strongly depends on the choice of

the auxiliary density  $g$ . It is well known that the optimal choice for  $g$  is (Bucklew (2013))

$$g^*(\mathbf{x}) = \frac{\phi(\mathbf{x})f(\mathbf{x})}{E}, \quad \mathbf{x} \in \mathbb{R}^n.$$

Indeed, for this choice we have  $\phi L = E$  and so  $\hat{E}_N$  is actually the deterministic estimator  $E$ . For this reason,  $g^*$  is sometimes called zero-variance density, a terminology that we will adopt here. Of course,  $g^*$  is only of theoretical interest as it depends on the unknown integral  $E$ . However, it gives an idea of good choices for the auxiliary density  $g$ , and we will seek to approximate  $g^*$  by an auxiliary density that minimizes the distance between  $g^*$  and a given parametric family of densities.

In this paper, the parametric family of densities is the Gaussian family  $\{g_{\mathbf{m},\Sigma} : \mathbf{m} \in \mathbb{R}^n, \Sigma \in \mathcal{S}_n^+\}$ , where  $g_{\mathbf{m},\Sigma}$  denotes the Gaussian density with mean  $\mathbf{m} \in \mathbb{R}^n$  and covariance matrix  $\Sigma \in \mathcal{S}_n^+$  with  $\mathcal{S}_n^+ \subset \mathbb{R}^{n \times n}$  the set of symmetric, positive-definite matrices:

$$g_{\mathbf{m},\Sigma}(\mathbf{x}) = \frac{1}{\sqrt{(2\pi)^n \det(\Sigma)}} \exp\left(-\frac{1}{2}(\mathbf{x} - \mathbf{m})^\top \Sigma^{-1}(\mathbf{x} - \mathbf{m})\right), \quad \mathbf{x} \in \mathbb{R}^n.$$

Moreover, we will consider the Kullback–Leibler (KL) divergence to measure a “distance” between  $g^*$  and  $g_{\mathbf{m},\Sigma}$ . Recall that for two densities  $f$  and  $h$ , with  $f$  absolutely continuous with respect to  $h$ , the KL divergence  $D(f, h)$  between  $f$  and  $h$  is defined by:

$$D(f, h) = \mathbb{E}_f \left[ \log \left( \frac{f(\mathbf{X})}{h(\mathbf{X})} \right) \right] = \int \log \left( \frac{f(\mathbf{x})}{h(\mathbf{x})} \right) f(\mathbf{x}) d\mathbf{x}.$$

Thus, our goal is to approximate  $g$  by  $g_{\mathbf{m}^*,\Sigma^*}$  with the optimal mean vector  $\mathbf{m}^*$  and the optimal covariance matrix  $\Sigma^*$  given by (Rubinstein and Kroese (2011, 2017)) :

$$(\mathbf{m}^*, \Sigma^*) = \arg \min \{D(g^*, g_{\mathbf{m},\Sigma}) : \mathbf{m} \in \mathbb{R}^n, \Sigma \in \mathcal{S}_n^+\}. \quad (2)$$

In the Gaussian case of the present setting, it is well-known that  $\mathbf{m}^*$  and  $\Sigma^*$  are simply the mean and variance of the zero-variance density:

$$\mathbf{m}^* = \mathbb{E}_{g^*}(\mathbf{X}) \quad \text{and} \quad \Sigma^* = \text{Var}_{g^*}(\mathbf{X}). \quad (3)$$

### 3 Main result

#### 3.1 Projecting on a low dimensional subspace

As  $g^*$  is unknown (although sometimes we can sample from it, as will be considered below), the optimal parameters  $\mathbf{m}^*$  and  $\Sigma^*$  given by (3) are not directly computable. Therefore, usual estimation schemes start with estimating  $\mathbf{m}^*$  and  $\Sigma^*$ , say through  $\hat{\mathbf{m}}^*$  and  $\hat{\Sigma}^*$ , respectively, and then use these approximations to estimate  $E$  through (1) with the auxiliary density  $g = g_{\hat{\mathbf{m}}^*,\hat{\Sigma}^*}$ . Although the estimation of  $E$  with the auxiliary density  $g_{\hat{\mathbf{m}}^*,\hat{\Sigma}^*}$  usually provides very good results, it is well-known that in high dimension, the additional error induced by the estimations of  $\mathbf{m}^*$  and  $\Sigma^*$  severely degrades the accuracy of the final estimation (Uribe et al. (2020); Papaioannou et al. (2019)). The main problem lies in the estimation of  $\Sigma^*$  which, in dimension  $n$ , involves the estimation of a quadratic (in the dimension) number of terms, namely  $n(n+1)/2$ .

Recently, the idea to overcome this problem by only evaluating variance terms in a small number of influential directions was explored in Uribe et al. (2020) and El Masri et al. (2020). In these two papers, the covariance matrix  $\Sigma$  is modeled in the form

$$\Sigma = \sum_{i=1}^k (v_i - 1) \mathbf{d}_i \mathbf{d}_i^\top + I_n \quad (4)$$

where the  $\mathbf{d}_i$ 's are the  $k$  orthonormal directions which are deemed influential. It is easy to check that  $\Sigma$  is the covariance matrix of the Gaussian vector

$$v_1^{1/2}Y_1\mathbf{d}_1 + \dots + v_k^{1/2}Y_k\mathbf{d}_k + Y_{k+1}\mathbf{d}_{k+1} + \dots + Y_n\mathbf{d}_n$$

where the  $Y_i$ 's are i.i.d. standard normal random variables (one-dimensional), and the  $n - k$  vectors  $(\mathbf{d}_{k+1}, \dots, \mathbf{d}_n)$  complete  $(\mathbf{d}_1, \dots, \mathbf{d}_k)$  into an orthonormal basis. In particular,  $v_i$  is the variance in the direction of  $\mathbf{d}_i$ , i.e.,  $v_i = \mathbf{d}_i^\top \Sigma \mathbf{d}_i$ . In (4),  $k$  can be considered as the effective dimension in which variance terms are estimated. In other words, in [Uribe et al. \(2020\)](#) and [El Masri et al. \(2020\)](#), the optimal variance parameter is not sought in  $\mathcal{S}_n^+$  as in (2), but rather in the subset of matrices of the form

$$\mathcal{L}_{n,k} = \left\{ \sum_{i=1}^k (\alpha_i - 1) \frac{\mathbf{d}_i \mathbf{d}_i^\top}{\|\mathbf{d}_i\|^2} + I_n : \alpha_1, \dots, \alpha_k > 0 \text{ and the } \mathbf{d}_i \text{'s are orthogonal} \right\}.$$

The relevant minimization problem thus becomes

$$\Sigma_k^* = \arg \min \{D(g^*, g_{\mathbf{m}^*, \Sigma}) : \Sigma \in \mathcal{L}_{n,k}\} \quad (5)$$

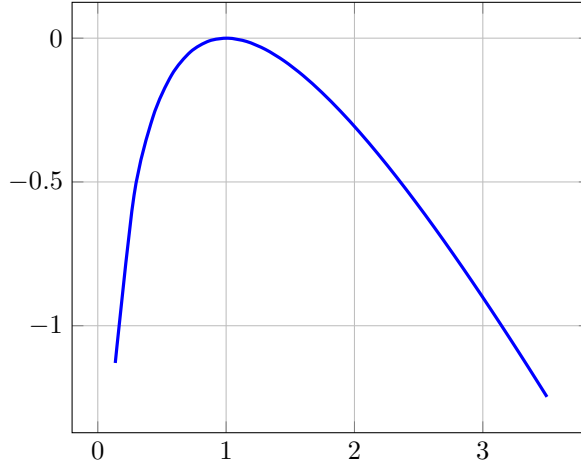
instead of (2), with the effective dimension  $k$  being allowed to be adjusted dynamically (see the proof of [Theorem 1](#) for a justification of considering  $\mathbf{m}^*$  instead of optimizing in  $\mathbf{m}$  also). By restricting the space in which the variance is looked up, one seeks to limit the number of variance terms to be estimated. The idea is that if the directions are suitably chosen, then the improvement of the accuracy due to the smaller error in estimating the variance terms will compensate the fact that we consider less candidates for the covariance matrix.

In [El Masri et al. \(2020\)](#), the authors consider  $k = 1$  and  $\mathbf{d}_1 = \mathbf{m}^* / \|\mathbf{m}^*\|$ . This choice is motivated by the fact that, due to the light tail of the Gaussian random variable and the reliability context, the variance should vary significantly in the direction of  $\mathbf{m}^*$  and so estimating the variance in this direction can bring information. The method in [Uribe et al. \(2020\)](#) is more involved:  $k$  is adjusted dynamically, while the directions  $\mathbf{d}_i$  are the eigenvectors associated to the largest eigenvalues of a certain matrix. They span a low-dimensional subspace called Failure-Informed Subspace, and the authors in [Uribe et al. \(2020\)](#) prove that this choice minimizes an **upper bound** on the minimal KL divergence. In practice, this algorithm yields very accurate results. However, we will not consider it further in the present paper for two reasons. First, this algorithm is tailored for the reliability case where  $\phi = \mathbb{I}_{\{\varphi \geq 0\}}$ , whereas our method is more general and applies to the general problem of estimating an integral (see for instance our test case of [Section 5.4](#)). Second, the algorithm in [Uribe et al. \(2020\)](#) requires the evaluation of the gradient of the function  $\varphi$ . However, this gradient is not always known and can be expensive to evaluate; in some cases, the function  $\varphi$  is even not differentiable, as will be the case in our numerical example in [Section 5.3](#). In contrast, our method makes no assumption on the form or smoothness of  $\phi$ : it needs not compute its gradient, and actually works even if it is not differentiable. For completeness, we have run the algorithm of [Uribe et al. \(2020\)](#) whenever applicable, and found that it outperformed our algorithm (see [Remark 1](#) below). Thus, whenever  $\phi$  is of the form  $\phi = \mathbb{I}_{\{\varphi \geq 0\}}$  with  $\varphi$  differentiable and its gradient available, then the algorithm of [Uribe et al. \(2020\)](#) seems preferable to ours. However, our aim here is to consider a more general setting.

### 3.2 Main result and positioning of the paper

The main result of the present paper is to actually compute the exact value for  $\Sigma_k^*$  in (5), which therefore paves the way for efficient high-dimensional estimation schemes. The statement of our result involves the following function  $\ell$ , which is represented in [Figure 1](#):

$$\ell : x \in (0, \infty) \mapsto \log(x) - x + 1. \quad (6)$$

Fig. 1: Plot of the function  $\ell(x) = \log x - x + 1$  given by (6).**Algorithm 1:** Algorithm suggested by Theorem 1.**Data:** Sample sizes  $N$  and  $M$ **Result:** Estimation  $\hat{E}_N$  of integral  $E$ 

- 1 Generate a sample  $\mathbf{X}_1, \dots, \mathbf{X}_M$  on  $\mathbb{R}^n$  independently according to  $g^*$
- 2 Estimate  $\hat{\mathbf{m}}^*$  and  $\hat{\Sigma}^*$  defined in (8) and (9) with this sample;
- 3 Compute the eigenpairs  $(\hat{\lambda}_i^*, \hat{\mathbf{d}}_i^*)$  of  $\hat{\Sigma}^*$  ranked in increasing  $\ell$ -order;
- 4 Compute the matrix  $\hat{\Sigma}_k^* = \sum_{i=1}^k (\hat{\lambda}_i^* - 1) \hat{\mathbf{d}}_i^* (\hat{\mathbf{d}}_i^*)^\top + I_n$  with  $k$  obtained by applying Algorithm 2 with input  $(\hat{\lambda}_1^*, \dots, \hat{\lambda}_n^*)$ ;
- 5 Generate a new sample  $\mathbf{X}_1, \dots, \mathbf{X}_N$  independently from  $g_{\hat{\mathbf{m}}^*, \hat{\Sigma}_k^*}$ ;
- 6 Return  $\hat{E}_N = \frac{1}{N} \sum_{i=1}^N \phi(\mathbf{X}_i) \frac{f(\mathbf{X}_i)}{\hat{g}(\mathbf{X}_i)}$  with  $\hat{g} = g_{\hat{\mathbf{m}}^*, \hat{\Sigma}_k^*}$ .

In the following,  $(\lambda, \mathbf{d}) \in \mathbb{R} \times \mathbb{R}^n$  is an eigenpair of a matrix  $A$  if  $A\mathbf{d} = \lambda\mathbf{d}$  and  $\|\mathbf{d}\| = 1$ . A diagonalizable matrix has  $n$  distinct eigenpairs, say  $((\lambda_i^*, \mathbf{d}_i^*), i = 1, \dots, n)$ , and we say that these eigenpairs are ranked in increasing  $\ell$ -order if  $\ell(\lambda_1^*) \leq \dots \leq \ell(\lambda_n^*)$ .

**Theorem 1** *Let  $(\lambda_i^*, \mathbf{d}_i^*)$  be the eigenpairs of  $\Sigma^*$  ranked in increasing  $\ell$ -order. Then for  $1 \leq k \leq n$ , the solution  $\Sigma_k^*$  to (5) is given by*

$$\Sigma_k^* = I_n + \sum_{i=1}^k (\lambda_i^* - 1) \mathbf{d}_i^* (\mathbf{d}_i^*)^\top. \quad (7)$$

For  $k = 1$  for instance, the shape of the function  $\ell$  depicted in Figure 1 implies that  $\Sigma_1^* = I_n + (\lambda^* - 1) \mathbf{d}^* (\mathbf{d}^*)^\top$  with  $(\lambda^*, \mathbf{d}^*)$  the eigenpair of  $\Sigma^*$  with  $\lambda^*$  either the largest or the smallest eigenvalue of  $\Sigma^*$ , depending on which one minimizes  $\ell$ .

This theoretical result therefore suggests to reduce dimension by estimating eigenpairs of  $\Sigma^*$ , rank them in increasing  $\ell$ -order and then use the  $k$  first eigenpairs  $((\lambda_i^*, \mathbf{d}_i^*), i = 1, \dots, k)$  to build the covariance matrix  $\hat{\Sigma}_k^* = \sum_{i=1}^k (\hat{\lambda}_i^* - 1) \hat{\mathbf{d}}_i^* (\hat{\mathbf{d}}_i^*)^\top + I_n$  and use it for the auxiliary density. This scheme is summarized in Algorithm 1 (the effective dimension  $k$  is obtained by Algorithm 2, see Section 3.3 below). As mentioned above, we assume in the first step of Algorithm 1 that we can sample according

| Direction       | $\mathbf{d}_i^*$                                 | $\mathbf{m}^*$                |
|-----------------|--|-------------------------------|
| Perfectly known | $\hat{\Sigma}_{\mathbf{d}}^*$                    | $\hat{\Sigma}_{\mathbf{m}}^*$ |
| Estimated       | $\hat{\Sigma}_{\mathbf{d}}^* = \hat{\Sigma}_k^*$ | $\hat{\Sigma}_{\mathbf{m}}^*$ |

Table 1: The four covariance matrices using projection studied in this paper. All these covariance matrices are of the form  $\sum_i (v_i - 1) \mathbf{d}_i \mathbf{d}_i^\top + I_n$  with  $v_i = \mathbf{d}_i^\top \hat{\Sigma}^* \mathbf{d}_i$ . Four choices are considered for the  $\mathbf{d}_i$ 's:  $\mathbf{d}_1 = \mathbf{m}^* / \|\mathbf{m}^*\|$  (perfectly known or estimated) and  $\mathbf{d}_i = \mathbf{d}_i^*$  of Theorem 1 (perfectly known or estimated). For instance, comparing the numerical results between  $\hat{\Sigma}_{\mathbf{d}}^*$  and  $\hat{\Sigma}_{\mathbf{m}}^*$  allows to assess which directions between the  $\mathbf{d}_i^*$ 's and  $\mathbf{m}^*$  are more promising, whereas comparing the numerical results between  $\hat{\Sigma}_{\mathbf{d}}^*$  and  $\hat{\Sigma}_{\mathbf{d}}^*$  allows to assess the error induced by estimating the  $\mathbf{d}_i^*$ 's.

to  $g^*$ . Since  $g^*$  is known up to a multiplicative constant, this is a reasonable assumption as classical techniques such as importance sampling with self-normalized weights or MCMC can be used in this case (see for instance Chan and Kroese (2012); Grace et al. (2014)). In this paper, this is done thanks to a basic rejection method that yields perfect samples, possibly at the price of a high computational cost. The primary goal of this paper is to understand whether the  $\mathbf{d}_i^*$ 's are indeed good projection directions, see the discussion below, and so this computational cost is not taken into account. Possible improvements to relax this assumption are discussed in the conclusion of the paper.

In this paper, we therefore estimate the  $(\lambda_i^*, \mathbf{d}_i^*)$ 's by computing the eigenpairs of the empirical estimation  $\hat{\Sigma}^*$  of  $\Sigma^*$  given by

$$\hat{\Sigma}^* = \frac{1}{M} \sum_{i=1}^M (\mathbf{X}_i - \hat{\mathbf{m}}^*)(\mathbf{X}_i - \hat{\mathbf{m}}^*)^\top \quad (8)$$

where

$$\hat{\mathbf{m}}^* = \frac{1}{M} \sum_{i=1}^M \mathbf{X}_i \quad (9)$$

is the empirical mean under  $g^*$  (which is a consistent estimator of  $\mathbf{m}^*$ ) and the  $\mathbf{X}_1, \dots, \mathbf{X}_M$  are i.i.d. random samples from  $g^*$  ( $M = 500$  for the estimation of  $\hat{\Sigma}^*$  in the tables in Section 5).

This choice is driven by the main objective of the present paper, which is to **get benchmark results to assess the efficiency of the proposed directions  $\mathbf{d}_i^*$** . The algorithm that we study here (Algorithms 1+2) aims at understanding whether:

1. projecting can improve the situation with respect to using  $\hat{\Sigma}^*$ ;
2. the  $\mathbf{d}_i^*$ 's are good candidates, in particular compared to the choice  $\mathbf{m}^*$  suggested in El Masri et al. (2020);
3. what is the impact in making errors in estimating the eigenpairs  $(\lambda_i^*, \mathbf{d}_i^*)$ .

To that end, in our numerical test cases we will compare six different choices for the covariance matrix:

1.  $\Sigma^*$ : the optimal covariance matrix given by (3);
2.  $\hat{\Sigma}^*$ : the empirical estimation of  $\Sigma^*$  given by (8).

These two choices will serve as benchmark:  $\Sigma^*$  will give optimal results, while results for  $\hat{\Sigma}^*$  will deteriorate as the dimension increases, which is the well-known behavior which we try to improve. We will then consider four other covariance matrices using different projection directions. The goal is to see whether one can improve estimations by projecting  $\hat{\Sigma}^*$  in suitable directions, so in each of the four cases, we will consider matrices which are of the form  $\sum_i (v_i - 1) \mathbf{d}_i \mathbf{d}_i^\top + I_n$  with  $v_i = \mathbf{d}_i^\top \hat{\Sigma}^* \mathbf{d}_i$ . The four choices  $\hat{\Sigma}_{\mathbf{d}}^*$ ,  $\hat{\Sigma}_{\mathbf{d}}^* = \hat{\Sigma}_k^*$ ,  $\hat{\Sigma}_{\mathbf{m}}^*$  and  $\hat{\Sigma}_{\mathbf{m}}^*$  are presented in Table 1 and its caption. They are obtained by a combination of two choices: the projection direction (the  $\mathbf{d}_i^*$ 's or  $\mathbf{m}^*$ ) and whether the directions are perfectly known or estimated. More precisely:

**Algorithm 2:** Choice of the number of dimensions**Data:** Sequence of positive numbers  $\lambda_1, \dots, \lambda_n$  in increasing  $\ell$ -order**Result:** Number of selected dimensions  $k$ 

- 1 Compute the increments  $\delta_i = \ell(\lambda_{i+1}) - \ell(\lambda_i)$  for  $i = 1 \dots n - 1$ ;
- 2 Return  $k = \arg \max \delta_i$ , the index of the maximum of the differences.

3.  $\hat{\Sigma}_{\mathbf{d}}^*$  is obtained by choosing  $\mathbf{d}_i = \mathbf{d}_i^*$  of Theorem 1, which is supposed to be perfectly known;
4.  $\hat{\Sigma}_{\mathbf{d}}^* = \hat{\Sigma}_k^*$  is obtained by choosing  $\mathbf{d}_i = \hat{\mathbf{d}}_i^*$  the eigenvector of  $\hat{\Sigma}^*$ , which is an estimation of  $\mathbf{d}_i^*$ ;
5.  $\hat{\Sigma}_{\mathbf{m}}^*$  is obtained by choosing  $k = 1$  and  $\mathbf{d}_1 = \mathbf{m}^* / \|\mathbf{m}^*\|$ , which is supposed to be perfectly known;
6.  $\hat{\Sigma}_{\mathbf{m}}^*$  is obtained by choosing  $k = 1$  and  $\mathbf{d}_1 = \hat{\mathbf{m}}^* / \|\hat{\mathbf{m}}^*\|$ , where  $\hat{\mathbf{m}}^*$  given by (9) is an estimation of  $\mathbf{m}^*$ .

For the two choices  $\hat{\Sigma}_{\mathbf{d}}^*$  and  $\hat{\Sigma}_{\mathbf{d}}^* = \hat{\Sigma}_k^*$ , the number of directions  $k$  is fixed by Algorithm 2. Moreover, for  $\hat{\Sigma}_{\mathbf{d}}^*$  and  $\hat{\Sigma}_{\mathbf{m}}^*$ , the projection directions, if not known analytically, are obtained by a brute force Monte Carlo scheme with a very high simulation budget as  $\mathbf{m}^*$  and  $\Sigma^*$  are unknown. Finally, we emphasize that Algorithm 1 corresponds to estimating and projecting on the  $\mathbf{d}_i^*$ 's, which is why the matrix  $\hat{\Sigma}_k^*$  of Algorithm 1 is equal to the matrix  $\hat{\Sigma}_{\mathbf{d}}^*$ , i.e.,  $\hat{\Sigma}_k^* = \hat{\Sigma}_{\mathbf{d}}^*$ . This redundant notation is motivated by the fact that  $\hat{\Sigma}_k^*$  emphasizes that one seeks to estimate  $\Sigma_k^*$  of Theorem 1, while  $\hat{\Sigma}_{\mathbf{d}}^*$  emphasizes that  $\hat{\Sigma}_k^*$  can be embedded in a larger class of covariance matrices: this viewpoint is useful as it makes it possible to disentangle the errors induced by the various steps of the algorithm.

3.3 Choice of the number of dimensions  $k$ 

The choice of the effective dimension  $k$ , i.e., the number of projection directions considered, is important. If it is close to  $n$ , then the matrix  $\hat{\Sigma}_k^*$  will be close to  $\hat{\Sigma}^*$  which is the situation we want to improve in the first place. On the other hand, setting  $k = 1$  in all cases may be too simple and lead to suboptimal results. In practice however, this is often a good choice. In order to adapt  $k$  dynamically, we consider a simple method based on the value of the KL divergence. Given the eigenvalues  $\lambda_1, \dots, \lambda_n$  ranked in increasing  $\ell$ -order, we look for the maximal gap in the sequence  $(\ell(\lambda_1), \dots, \ell(\lambda_n))$ . This allows to chose  $k$  such that  $\sum_{i=1}^k \ell(\lambda_i)$  is close to  $\sum_{i=1}^n \ell(\lambda_i)$  which is equal, up to an additive constant, to the minimal KL divergence (see (12) below). The precise method is described in Algorithm 2.

## 4 Proof of Theorem 1

For any  $\mathbf{m} \in \mathbb{R}^n$  and  $\Sigma \in \mathcal{S}_n^+$ , we have by definition

$$\begin{aligned}
D(g^*, g_{\mathbf{m}, \Sigma}) &= \mathbb{E}_{g^*} \left( \log \left( \frac{g^*(\mathbf{X})}{g_{\mathbf{m}, \Sigma}(\mathbf{X})} \right) \right) \\
&= \mathbb{E}_{g^*} \left( \log \left( \frac{\phi(\mathbf{X}) g_{0, I_n}(\mathbf{X})}{E g_{\mathbf{m}, \Sigma}(\mathbf{X})} \right) \right) \\
&= \mathbb{E}_{g^*} \left( \log \left( \frac{\phi(\mathbf{X})}{E} \right) + \frac{1}{2} \log \det(\Sigma) + \frac{1}{2} (\mathbf{X} - \mathbf{m})^\top \Sigma^{-1} (\mathbf{X} - \mathbf{m}) - \frac{1}{2} \mathbf{X}^\top \mathbf{X} \right).
\end{aligned}$$

The gradient in  $\mathbf{m}$  is equal to  $\Sigma^{-1} \mathbb{E}_{g^*}(\mathbf{X} - \mu)$ . This implies that the function is necessarily minimized in  $\mathbf{m} = \mathbf{m}^*$ , which will be assumed for the rest of the proof (and also justifies setting  $\mathbf{m} = \mathbf{m}^*$  in (5)).

The terms  $\mathbb{E}_g \log(\phi(\mathbf{X})/E)$  and  $\mathbb{E}_g \mathbf{X}^\top \mathbf{X}$  being independent of  $\Sigma$ , in the rest of the proof (and of the paper) we will focus on the remaining terms and define

$$D'(\Sigma) = \log \det \Sigma + \mathbb{E}_{g^*} \left( (\mathbf{X} - \mathbf{m}^*)^\top \Sigma^{-1} (\mathbf{X} - \mathbf{m}^*) \right).$$

Using the identity  $a^\top b = \text{tr}(ab^\top)$  for any two column vectors, we see that

$$\mathbb{E}_{g^*} \left[ (\mathbf{X} - \mathbf{m}^*)^\top \Sigma^{-1} (\mathbf{X} - \mathbf{m}^*) \right] = \mathbb{E}_{g^*} \left[ \text{tr} \left( (\mathbf{X} - \mathbf{m}^*) (\mathbf{X} - \mathbf{m}^*)^\top \Sigma^{-1} \right) \right].$$

Since the expectation and trace operators commute, using the linearity of the expectation and the fact that  $\Sigma^* = \text{Var}_{g^*}(\mathbf{X})$ , we finally obtain

$$D'(\Sigma) = \log \det \Sigma + \text{tr}(\Sigma^* \Sigma^{-1}). \quad (10)$$

The goal is to minimize this quantity over  $\Sigma \in \mathcal{L}_{n,k}$ . In the rest of the proof, we consider  $\mathbf{v} = (v_1, \dots, v_k) \in (0, \infty)^k$  and  $\mathbf{d} = (\mathbf{d}_1, \dots, \mathbf{d}_k)$  orthogonal, and we are interested in minimizing  $D'(\Sigma)$  with  $\Sigma = \sum_{i=1}^k (v_i - 1) \mathbf{d}_i \mathbf{d}_i^\top / \|\mathbf{d}_i\|^2 + I_n$ . Thus, in the sequel, we see  $D'$  as a function of  $\mathbf{v}$  and  $\mathbf{d}$ .

*First step: computation of  $D'(\Sigma)$ .* The goal of this first step is to prove that

$$D'(\Sigma) = D'(\mathbf{v}, \mathbf{d}) = \sum_{i=1}^k \left[ \log(v_i) + \left( \frac{1}{v_i} - 1 \right) \psi(\mathbf{d}_i) \right] + \text{tr}(\Sigma^*) \quad (11)$$

where here and in the sequel,  $\Sigma = \sum_{i=1}^k (v_i - 1) \mathbf{d}_i \mathbf{d}_i^\top / \|\mathbf{d}_i\|^2 + I_n$  and  $\psi(\mathbf{x}) = \mathbf{x}^\top \Sigma^* \mathbf{x} / \|\mathbf{x}\|^2$ . To do so, note that  $\Sigma = Q \Delta Q^\top$ , with  $\Delta = \text{diag}(v_1, \dots, v_k, 1, \dots, 1)$  a diagonal matrix and  $Q$  an orthogonal matrix with  $\mathbf{d}_i / \|\mathbf{d}_i\|$  as  $k$  first columns. Indeed, we have  $\Sigma \mathbf{d}_i = v_i \mathbf{d}_i$ , so that  $\mathbf{d}_i$  is an eigenvector with eigenvalue  $v_i$ . Moreover, for all  $\mathbf{d}_\perp$  in the orthogonal space of  $\text{span}(\mathbf{d})$ , we have  $\Sigma \mathbf{d}_\perp = \mathbf{d}_\perp$ , so that 1 is eigenvalue of multiplicity  $n - k$  (or more if some of the  $v_i$ 's are equal to one).

It follows from this decomposition that  $\det(\Sigma) = v_1 \cdots v_k$ . Moreover, we have

$$\text{tr}(\Sigma^* \Sigma^{-1}) = \text{tr}(\Sigma^* Q \Delta^{-1} Q^\top) = \text{tr}(\Delta^{-1} Q^\top \Sigma^* Q).$$

Since the first columns of  $Q$  are  $\mathbf{d}_i / \|\mathbf{d}_i\|$ , the first diagonal coefficients of  $Q^\top \Sigma^* Q$  are  $\psi(\mathbf{d}_i)$ . Thus, if  $\mathbf{d}_{k+1}, \dots, \mathbf{d}_n$  complete the  $\mathbf{d}_i / \|\mathbf{d}_i\|$  into an orthonormal basis, we have

$$\text{tr}(\Delta^{-1} Q^\top \Sigma^* Q) = \sum_{i=1}^k \frac{1}{v_i} \psi(\mathbf{d}_i) + \sum_{i=k+1}^n \psi(\mathbf{d}_i) = \sum_{i=1}^k \left( \frac{1}{v_i} - 1 \right) \psi(\mathbf{d}_i) + \sum_{i=1}^n \psi(\mathbf{d}_i).$$

Since the last sum  $\sum_{i=1}^n \psi(\mathbf{d}_i)$  is equal to  $\text{tr}(Q^\top \Sigma^* Q) = \text{tr}(\Sigma^*)$ , gathering the previous equalities leads to (11).

*Second step: minimization.* Starting from (11), we see that the derivative in  $v_i$  is given by

$$\frac{\partial D'}{\partial v_i}(\mathbf{v}, \mathbf{d}) = \frac{1}{v_i} - \frac{1}{v_i^2} \psi(\mathbf{d}_i) = \frac{1}{v_i^2} (v_i - \psi(\mathbf{d}_i)).$$

Thus, for fixed  $\mathbf{d}$ ,  $D'$  is decreasing in  $v_i$  for  $v_i < \psi(\mathbf{d}_i)$  and then increasing for  $v_i > \psi(\mathbf{d}_i)$ , which shows that, for fixed  $\mathbf{d}$ ,  $D'$  is minimized for  $v_i = \psi(\mathbf{d}_i)$ . For this value, say  $\mathbf{v}^* = (\psi(\mathbf{d}_1), \dots, \psi(\mathbf{d}_k))$  we have

$$D'(\mathbf{v}^*, \mathbf{d}) = \sum_{i=1}^k [\log(\psi(\mathbf{d}_i)) + 1 - \psi(\mathbf{d}_i)] + \text{tr}(\Sigma^*) = \sum_{i=1}^k \ell(\psi(\mathbf{d}_i)) + \text{tr}(\Sigma^*). \quad (12)$$

Since  $\ell$  is increasing and then decreasing, it is clear from this expression that in order to minimize  $D'$ , one must choose the  $\mathbf{d}_i$ 's in order to either maximize or minimize  $\psi$ , whichever minimizes  $\ell$ . Since the variational characterization of eigenvalues shows that eigenvectors precisely solve this problem, we get the desired result.



## 5 Numerical results

As explained above, we want to compare the accuracy of the auxiliary densities  $g_{\mathbf{m}^*, \Sigma}$  for the six choices of covariance matrix  $\Sigma$  introduced in Section 3.2. As we have seen in (10), the KL divergence is, up to an additive constant, equal to  $D'(\Sigma) = \log \det \Sigma + \text{tr}(\Sigma^* \Sigma^{-1})$  which we will refer to as partial KL divergence. In the following tables, we report the mean value of  $D'(\Sigma)$ , the corresponding relative error compared to the optimal  $D'(\Sigma^*)$ , the mean estimation (1) of the integral, the relative bias of this estimation and the corresponding coefficient of variation. The reported value of the partial KL divergence is an averaged value over 50 independent runs. The relative error of the KL divergence is computed through:

$$\text{Relative error} = \frac{D'(\Sigma) - D'(\Sigma^*)}{D'(\Sigma^*)}.$$

Note that this error is positive since  $D'(\Sigma^*)$  is the minimal partial KL divergence. The mean estimation is the average of 50 independent estimations of  $\hat{E}_N$ :

$$\text{Mean} = \frac{1}{50} \sum_{i=1}^{50} \hat{E}_N^{(i)},$$

with  $N = 2000$ . The relative bias and the coefficient of variation of the estimation are defined respectively as:

$$\text{Relative bias} = \frac{\text{Mean} - E}{E} \quad \text{and} \quad \text{Coefficient of variation} = \frac{1}{E} \sqrt{\frac{1}{50} \sum_{i=1}^{50} (\hat{E}_N^{(i)} - E)^2}$$

where the reference value  $E$  is estimated by a crude Monte Carlo method with a very large sample size when it is unknown theoretically.

### 5.1 Toy example 1: one-dimensional optimal projection

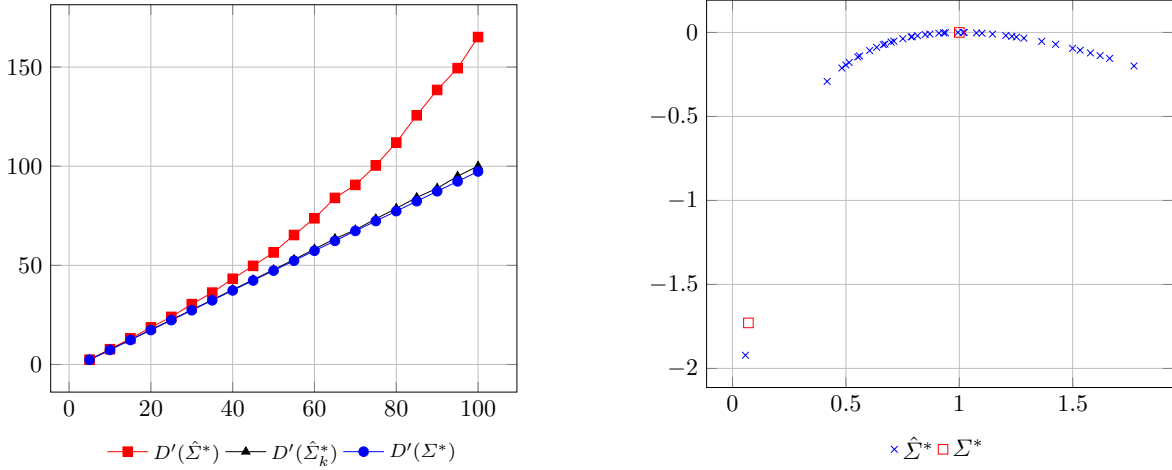
We consider a toy example where all computations can be made exactly. This is a classical example of rare event probability estimation, often used to test the robustness of a method in high dimension. It is given by  $\phi(\mathbf{x}) = \mathbb{I}_{\{\varphi(\mathbf{x}) \geq 0\}}$  with  $\varphi$  the following affine function:

$$\varphi : \mathbf{x} = (x_1, \dots, x_n) \in \mathbb{R}^n \mapsto \sum_{j=1}^n x_j - 3\sqrt{n}. \quad (13)$$

Here, the zero-variance density is  $g^*(\mathbf{x}) = \frac{f(\mathbf{x}) \mathbb{I}_{\{\varphi(\mathbf{x}) \geq 0\}}}{E}$ , which is a truncated standard Gaussian, with  $E = \mathbb{P}_f(\varphi(\mathbf{X}) \geq 0) \simeq 1.35 \cdot 10^{-3}$  for all  $n$ , and the optimal parameters  $\mathbf{m}^*$  and  $\Sigma^*$  in (3) can be computed exactly, namely  $\mathbf{m}^* = \alpha \mathbf{1}$  with  $\alpha = e^{-9/2} / (E(2\pi n)^{1/2})$  and  $\mathbf{1} = \frac{1}{\sqrt{n}}(1, \dots, 1) \in \mathbb{R}^n$  the normalized constant vector, and  $\Sigma^* = (v - 1)\mathbf{1}\mathbf{1}^\top + I_n$  with  $v = \frac{3}{\sqrt{n}}\alpha - \alpha^2 + 1$ .

#### 5.1.1 Evolution of the partial KL divergence and spectrum

Figure 2a represents the evolution as the dimension varies between 5 and 100 of the partial KL divergence  $D'$  for three different choices of covariance matrix: the optimal matrix  $\Sigma^*$ , its empirical estimation  $\hat{\Sigma}^*$  and the estimation  $\hat{\Sigma}_k^*$  of the optimal lower-dimensional covariance matrix. To compute  $\hat{\Sigma}^*$ , we generate a sample  $\mathbf{X}_1, \dots, \mathbf{X}_M$ , of size  $M = 200$  from  $g^*$  by acceptance-rejection method, for each dimension  $n$ . Then  $\hat{\Sigma}_k^*$  is estimated from  $\hat{\Sigma}^*$  following algorithm 1. We can notice that the partial



(a) Evolution of the partial KL divergence as the dimension increases, with the optimal covariance matrix  $\Sigma^*$  (blue circles), the sample covariance  $\hat{\Sigma}^*$  (red squares), and the projected covariance  $\hat{\Sigma}_k^*$  (black triangles).

(b) Computation of  $\ell(\lambda_i)$  for the eigenvalues of  $\Sigma^*$  (red squares) and  $\hat{\Sigma}^*$  (blue crosses) in dimension  $n = 40$ .

Fig. 2: Simulation results for the function  $\phi = \mathbb{I}_{\varphi \geq 0}$  with  $\varphi$  the linear function given by (13).

KL divergence for  $\hat{\Sigma}^*$  grows much faster than the other two, and that the partial KL divergence for  $\hat{\Sigma}_k^*$  remains very close to the optimal value  $D'(\Sigma^*)$ . As the KL divergence is a proxy for the efficiency of the auxiliary density (it is for instance closely related to the number of samples required for a given precision in Chatterjee and Diaconis (2018)), this suggests that using  $\hat{\Sigma}_k^*$  will provide results close to optimal.

We now check this claim. As  $\Sigma^* = (v-1)\mathbf{1}\mathbf{1}^\top + I_n$ , its eigenpairs are  $(v, \mathbf{1})$  and  $(1, \mathbf{d}_i)$  where the  $\mathbf{d}_i$ 's form an orthonormal basis of the space orthogonal to the space spanned by  $\mathbf{1}$ . In particular,  $(v, \mathbf{1})$  is the smallest (in  $\ell$ -order) eigenpair of  $\Sigma^*$  and  $\Sigma_k^* = \Sigma^*$  for any  $k \geq 1$ . In practice, we do not use this theoretical knowledge and  $\Sigma^*$ ,  $\Sigma_k^*$  and the eigenpairs are estimated as explained above. The six covariance matrices introduced in Section 3.2 and in which we are interested are as follows:

- $\Sigma^* = (v-1)\mathbf{1}\mathbf{1}^\top + I_n$ ;
- $\hat{\Sigma}^*$  given by (8);
- $\hat{\Sigma}_{\mathbf{m}}^*$  and  $\hat{\Sigma}_{\mathbf{d}}^*$  are equal and given by  $(\hat{\lambda}-1)\mathbf{1}\mathbf{1}^\top + I_n$  with  $\hat{\lambda} = \mathbf{1}^\top \hat{\Sigma}^* \mathbf{1}$ . This amounts to assuming that the projection direction  $\mathbf{1}$  is perfectly known, whereas the variance in this direction is estimated;
- $\hat{\Sigma}_{\mathbf{d}}^* = (\hat{\lambda}-1)\hat{\mathbf{d}}\hat{\mathbf{d}}^\top + I_n$  with  $(\hat{\lambda}, \hat{\mathbf{d}})$  the smallest eigenpair of  $\hat{\Sigma}^*$ . The difference with the previous case is that we do not assume anymore that the optimal projection direction  $\mathbf{1}$  is known. It therefore needs to be estimated, which is the purpose of  $\hat{\mathbf{d}}$ ;
- $\hat{\Sigma}_{\mathbf{m}}^* = (\hat{\lambda}-1)\frac{\hat{\mathbf{m}}^*(\hat{\mathbf{m}}^*)^\top}{\|\hat{\mathbf{m}}^*\|^2} + I_n$  with  $\hat{\mathbf{m}}^*$  given by (9) and  $\hat{\lambda} = \frac{(\hat{\mathbf{m}}^*)^\top \hat{\Sigma}^* \hat{\mathbf{m}}^*}{\|\hat{\mathbf{m}}^*\|^2}$ . Here we assume that  $\mathbf{m}^*$  is a good direction projection, but is unknown and therefore needs to be estimated.

Note that in the particularly simple case considered here, both  $\hat{\mathbf{m}}^*/\|\hat{\mathbf{m}}^*\|$  and  $\hat{\mathbf{d}}$  are estimators of  $\mathbf{1}$  but they are obtained by different methods. In the next example we will consider a case where  $\mathbf{m}^*$  is not an optimal projection direction as given by Theorem 1.

Figure 2b represents the images by  $\ell$  of the eigenvalues of  $\Sigma^*$  and  $\hat{\Sigma}^*$ . **This picture carries a very important insight.** We see that the estimation of most eigenvalues is poor: indeed, all the blue crosses except the leftmost one are meant to be estimator of 1, whereas we see that they are more or less uniformly spread between 0.4 and 1.8. This means that the variance terms in the corresponding directions are poorly estimated, which could be the explanation on why the use of

|           |                              | $\Sigma^*$ | $\hat{\Sigma}^*$ | $\hat{\Sigma}_{\mathbf{m}}^* = \hat{\Sigma}_{\mathbf{d}}^*$ | $\hat{\Sigma}_{\mathbf{d}}^*$ | $\hat{\Sigma}_{\mathbf{m}}^*$ |
|-----------|------------------------------|------------|------------------|---|-------------------------------|-------------------------------|
| $n = 40$  | $D'(\Sigma)$                 | 37.35      | 39.25            | 37.35   | 37.45                         | 37.43                         |
|           | Relative error (%)           | 0          | 5.0              | 0.02  | 0.27                          | 0.21                          |
|           | Mean ( $\times 10^{-3}$ )    | 1.354      | 1.339            | 1.335   | 1.338                         | 1.347                         |
|           | Relative bias (%)            | 0.30       | -0.82            | -1.1  | -0.87                         | -0.23                         |
|           | Coefficient of variation (%) | 2.7        | 9.4              | 2.7   | 2.5                           | 2.0                           |
| $n = 70$  | $D'(\Sigma)$                 | 67.35      | 73.77            | 67.35   | 67.57                         | 67.50                         |
|           | Relative error (%)           | 0          | 9.5              | 0.01  | 0.33                          | 0.22                          |
|           | Mean ( $\times 10^{-3}$ )    | 1.349      | 1.325            | 1.340   | 1.349                         | 1.352                         |
|           | Relative bias (%)            | -0.08      | -1.9             | -0.71   | -0.05                         | 0.17                          |
|           | Coefficient of variation (%) | 2.0        | 35               | 2.4   | 3.4                           | 2.4                           |
| $n = 100$ | $D'(\Sigma)$                 | 97.35      | 111.91           | 97.36   | 97.73                         | 97.55                         |
|           | Relative error (%)           | 0          | 15.0             | 0.01  | 0.39                          | 0.21                          |
|           | Mean ( $\times 10^{-3}$ )    | 1.342      | 1.002            | 1.346   | 1.350                         | 1.345                         |
|           | Relative bias (%)            | -0.62      | -26              | -0.31   | 0.01                          | -0.35                         |
|           | Coefficient of variation (%) | 2.5        | 90               | 2.3   | 5.1                           | 3.7                           |

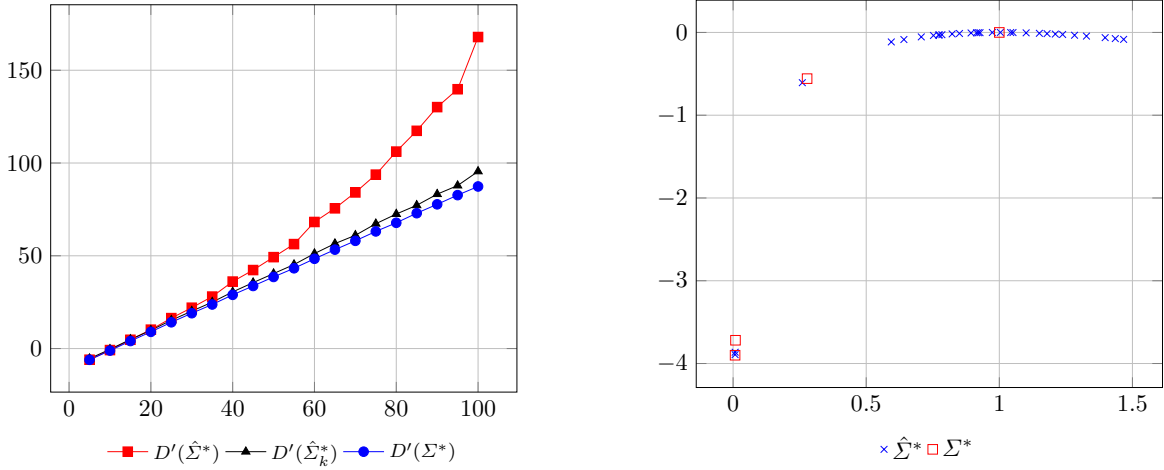
Table 2: Numerical comparison of the estimation of  $E$  considering the six covariance matrices of Section 3.2 when  $\phi = \mathbb{I}_{\{\varphi \geq 0\}}$  with  $\varphi$  the linear function given by (13). We seek to improve the results given by  $\hat{\Sigma}^*$ . In the third column  $\hat{\Sigma}_{\mathbf{m}}^* = \hat{\Sigma}_{\mathbf{d}}^*$  only the variance is estimated, so comparing the third to the second column highlights the potential improvement by projecting. Comparing the last two columns ( $\hat{\Sigma}_{\mathbf{d}}^*$  and  $\hat{\Sigma}_{\mathbf{m}}^*$ ) to the third one emphasizes the influence of the error in estimating the projection direction.

$\hat{\Sigma}^*$  gives an inaccurate estimation. But what we see also is that the function  $\ell$  is quite flat around one: as a consequence, **although the eigenvalues offer significant variability, this variability is smoothed by the action of  $\ell$** . Indeed, the images of the eigenvalues by  $\ell$  take values between  $-0.4$  and  $0$  and have smaller variability. Moreover,  $\ell$  decreases sharply around  $0$  and thus efficiently distinguishes between the two leftmost estimated eigenvalues and is able to separate them.

### 5.1.2 Numerical results

We report in Table 2 the numerical results for the six different matrices for varying dimensions  $n = 40$ ,  $70$  and  $100$ . The column  $\Sigma^*$  gives the optimal results, while the column  $\hat{\Sigma}^*$  corresponds to the results that we are trying to improve. Comparing these two columns, we see as expected that the estimation of  $E$  with  $\hat{\Sigma}^*$  significantly degrades as the dimension increases, with relative bias around 25 % and coefficient of variation up to 90 % in dimension 100. Compared to the first column  $\Sigma^*$ , the third column  $\hat{\Sigma}_{\mathbf{m}}^* = \hat{\Sigma}_{\mathbf{d}}^*$  corresponds to the best direction projection  $\mathbf{1}$  (as for  $\Sigma^*$ ) but estimating the variance in this direction (instead of the true variance) with  $\mathbf{1}^\top \hat{\Sigma}^* \mathbf{1}$ . This choice performs very well, with numerical results similar to the optimal ones. This can be understood since in this case, both  $\hat{\Sigma}_{\mathbf{m}}^*$  and  $\Sigma^*$  are of the form  $\alpha \mathbf{1}\mathbf{1}^\top + I_n$  and so estimating  $\hat{\Sigma}_{\mathbf{m}}^*$  requires only a one-dimensional estimation (namely, the estimation of  $\alpha$ ). Next, the last two columns  $\hat{\Sigma}_{\mathbf{d}}^*$  and  $\hat{\Sigma}_{\mathbf{m}}^*$  highlight the impact of having to estimate the projection directions in addition to the variance since these two matrices are of the form  $\hat{\alpha} \hat{\mathbf{1}} \hat{\mathbf{1}}^\top + I_n$  with both  $\hat{\alpha}$  (the variance term) and  $\hat{\mathbf{1}}$  (the direction) being estimated. We observe that these matrices yield results which are close to optimal and greatly improve the estimation obtained using  $\hat{\Sigma}^*$ . In dimension 100 for instance, the relative bias and coefficient of variation are around 0.3 % and 4 % for  $\hat{\Sigma}_{\mathbf{m}}^*$ , and around 0.01 % and 5 % for  $\hat{\Sigma}_{\mathbf{d}}^*$ , compared to  $-0.6$  % and 2.5 % for  $\Sigma^*$ .

Moreover, we observe that  $\hat{\Sigma}_{\mathbf{m}}^*$  gives slightly better results than  $\hat{\Sigma}_{\mathbf{d}}^*$ . We suggest that this is because  $\hat{\mathbf{m}}^*/\|\hat{\mathbf{m}}^*\|$  is a better estimator of  $\mathbf{1}$  than the eigenvector of  $\hat{\Sigma}^*$ . Indeed, evaluating  $\hat{\mathbf{m}}^*$  requires the estimation of  $n$  parameters, whereas  $\hat{\Sigma}^*$  needs around  $n^2/2$  parameters to estimate, so the eigenvector is finally more noisy than the mean vector.



(a) Evolution of the partial KL divergence as the dimension increases, with the optimal covariance matrix  $\Sigma^*$  (blue circles), the sample covariance  $\hat{\Sigma}^*$  (red squares), and the projected covariance  $\hat{\Sigma}_k^*$  (black triangles).

(b) Computation of  $\ell(\lambda_i)$  for the eigenvalues of  $\Sigma^*$  (red squares) and  $\hat{\Sigma}^*$  (blue crosses) in dimension  $n = 30$ .

Fig. 3: Simulation results for the function  $\phi = \mathbb{I}_{\varphi \geq 0}$  with  $\varphi$  given by (14) in dimension  $n = 30$ . Left: same behavior as for the first toy example. Right: we now have two eigenvalues that stand out, and the behavior of  $\ell$  is such that Algorithm 2 selects  $k = 2$  which corresponds to the leftmost two.

Thus, the proposed idea improves significantly the probability estimation in high dimension. But we see that the method taken in El Masri et al. (2020) is at least as much efficient in this example where we need only a one-dimensional projection. The next case shows that the projection on more than one direction can outperform the one-dimensional projection on  $\mathbf{m}^*$ .

## 5.2 Toy example 2: projection in 2 directions

The second toy example is again a probability estimation, i.e., it is of the form  $\phi = \mathbb{I}_{\{\varphi \geq 0\}}$  with now the function  $\varphi$  having some quadratic terms:

$$\varphi : \mathbf{x} = (x_1, \dots, x_n) \in \mathbb{R}^n \mapsto x_1 - 25x_2^2 - 30x_3^2 - 1. \quad (14)$$

As will be discussed in more details in the conclusion, this function is motivated in part because  $\mathbf{m}^*$  and  $\mathbf{d}_1^*$  are different and also because Algorithm 2 chooses two projection directions. Thus, this is an example where  $\hat{\Sigma}_{\mathbf{m}}^*$  and  $\hat{\Sigma}_{\mathbf{d}}^*$  are significantly different, which contrasts with the other three examples considered.

### 5.2.1 Evolution of the partial KL divergence and spectrum

We check on Figure 3a that the partial KL divergence obeys the same behavior as for the previous example, namely the one associated with  $\hat{\Sigma}^*$  increases much faster than the ones associated with  $\Sigma^*$  and  $\hat{\Sigma}_k^*$ , which again suggests that projecting can improve the situation. Since the function  $\varphi$  only depends on the first three variables and is even in  $x_2$  and  $x_3$ , one gets that  $\mathbf{m}^* = \alpha \mathbf{e}_1$  with  $\alpha = \mathbb{E}(X_1 \mid X_1 \geq 25X_2^2 + 30X_3^2 + 1) \approx 1.9$  (here and in the sequel,  $\mathbf{e}_i$  denotes the  $i$ th canonical vector

|                                       |                              | $\Sigma^*$ | $\hat{\Sigma}^*$ | $\hat{\Sigma}_{\mathbf{d}}^*$ | $\hat{\Sigma}_{\mathbf{m}}^*$ | $\hat{\Sigma}_{\mathbf{d}}^*$ | $\hat{\Sigma}_{\mathbf{m}}^*$ |
|---------------------------------------|------------------------------|------------|------------------|-------------------------------|-------------------------------|-------------------------------|-------------------------------|
| $n = 30$<br>$E = 1.51 \cdot 10^{-3}$  | $D'(\Sigma)$                 | 19.10      | 20.15            | 19.67                         | 26.73                         | 19.81                         | 26.76                         |
|                                       | Relative error (%)           | 0          | 5.5              | 2.9                           | 39.9                          | 3.7                           | 40.1                          |
|                                       | Mean ( $\times 10^{-3}$ )    | 1.525      | 1.541            | 1.494                         | 1.426                         | 1.508                         | 1.453                         |
|                                       | Relative bias (%)            | 0.97       | 2.0              | -1.0                          | -5.6                          | -0.10                         | -3.8                          |
| $n = 70$<br>$E = 1.51 \cdot 10^{-3}$  | $D'(\Sigma)$                 | 59.11      | 65.58            | 59.68                         | 66.73                         | 60.08                         | 66.80                         |
|                                       | Relative error (%)           | 0          | 10.9             | 0.96                          | 12.9                          | 1.6                           | 13.0                          |
|                                       | Mean ( $\times 10^{-3}$ )    | 1.510      | 1.407            | 1.513                         | 1.517                         | 1.537                         | 1.555                         |
|                                       | Relative bias (%)            | 0.02       | -6.8             | 0.19                          | 0.46                          | 1.8                           | 2.9                           |
| $n = 100$<br>$E = 1.51 \cdot 10^{-3}$ | $D'(\Sigma)$                 | 89.11      | 103.69           | 89.68                         | 96.73                         | 90.35                         | 96.82                         |
|                                       | Relative error (%)           | 0          | 16.4             | 0.64                          | 8.6                           | 1.4                           | 8.7                           |
|                                       | Mean ( $\times 10^{-3}$ )    | 1.498      | 1.093            | 1.504                         | 1.512                         | 1.485                         | 1.484                         |
|                                       | Relative bias (%)            | -0.82      | -27.5            | -0.40                         | 0.15                          | -1.7                          | -1.7                          |
|                                       | Coefficient of variation (%) | 2.6        | 84               | 2.9                           | 25.1                          | 7.0                           | 21.9                          |

Table 3: Numerical comparison of the estimation of  $E$  using the six covariance matrices of Section 3.2 when  $\phi = \mathbb{1}_{\{\varphi \geq 0\}}$  with  $\varphi$  the quadratic function given by (14).

of  $\mathbb{R}^n$ , i.e., all its coordinates are 0 except the  $i$ -th one which is equal to one), and that  $\Sigma^*$  is diagonal with

$$\Sigma^* = \begin{pmatrix} \lambda_1 & 0 & 0 & 0 & \cdots & 0 \\ 0 & \lambda_2 & 0 & 0 & \cdots & 0 \\ 0 & 0 & \lambda_3 & 0 & \cdots & 0 \\ 0 & 0 & 0 & 1 & \cdots & 0 \\ \vdots & \vdots & \vdots & \vdots & \ddots & \vdots \\ 0 & 0 & 0 & 0 & \cdots & 1 \end{pmatrix}.$$

Note that the off-diagonal elements of the submatrix  $(\Sigma_{ij}^*)_{1 \leq i, j \leq 3}$  are indeed 0 since they amount to integrating an odd function of an odd random variable with an even conditioning. For instance, if  $F(x) = \mathbb{P}(30X_3^2 + 1 \leq x)$ , then by conditioning on  $(X_1, X_3)$  we obtain

$$\begin{aligned} \Sigma_{12}^* &= \mathbb{E}((X_1 - \alpha)X_2 \mid X_1 - 25X_2^2 \geq 30X_3^2 + 1) \\ &= \frac{1}{E} \mathbb{E}[(X_1 - \alpha)\mathbb{E}(X_2 F(X_1 - 25X_2^2) \mid X_1)] \end{aligned}$$

which is 0 as  $x_2 F(x_1 - x_2^2)$  is an odd function of  $x_2$  for fixed  $x_1$ , and  $X_2$  has an even density. We can numerically compute  $\lambda_1 \approx 0.278$ ,  $\lambda_2 \approx 0.009$  and  $\lambda_3 \approx 0.0075$ . These values correspond to the red squares in Figure 3b which shows that the smallest eigenvalues are properly estimated. Moreover, Algorithm 2 selects the two smallest eigenvalues, which have the smallest  $\ell$ -values. These two eigenvalues thus correspond to the eigenvectors  $\mathbf{e}_2$  and  $\mathbf{e}_3$ , and so we see that on this example, the optimal directions predicted by Theorem 1 are significantly different (actually, orthogonal) from  $\mathbf{m}^*$  which is proportional to  $\mathbf{e}_1$ .

### 5.2.2 Numerical results

The numerical results of our simulations are presented in Table 3. We remark as before that, when using  $\hat{\Sigma}^*$ , the accuracy quickly deteriorates as the dimension increases as shows the 84 % coefficient of variation in dimension  $n = 100$ . In contrast,  $\hat{\Sigma}_{\mathbf{d}}^*$  leads to very accurate results, which remain close to optimal up to the same dimension  $n = 100$ . This behavior is to compare with the evolution of the relative KL divergence: whereas for  $\hat{\Sigma}^*$ , the relative error increases from 5.5 to 16.4 % as the dimension increases from  $n = 30$  to 100,  $\hat{\Sigma}_{\mathbf{d}}^*$  gives a partial KL divergence close to optimal, with a relative error

less than 1 % in dimension  $n = 100$ . This confirms that the KL divergence is indeed a good proxy to assess the relevance of an auxiliary density.

It is also interesting to note that the direction  $\mathbf{m}^*$  improves the situation compared to not projecting (column  $\hat{\Sigma}_{\mathbf{m}}^*$  compared to  $\hat{\Sigma}^*$ ), but using  $\hat{\Sigma}_{\mathbf{d}}^*$  gives significantly better results, with for instance a coefficient of variation around 3 % for  $\hat{\Sigma}_{\mathbf{d}}^*$  and around 25 % for  $\hat{\Sigma}_{\mathbf{m}}^*$  in dimension  $n = 100$ . Thus, this confirms our theoretical result that the  $\mathbf{d}_i^*$ 's are good directions on which to project.

Finally, we note that performing estimations of the projection directions instead of taking the true ones (column  $\hat{\Sigma}_{\mathbf{d}}^*$  vs  $\hat{\Sigma}_{\mathbf{d}}^*$ ) slightly degrades the situation, making the coefficient of variation increase from 3 to 7 % in dimension 100 for instance. However, the accuracy remains satisfactory as the dimension increases, as the coefficient of variation increases from 4 % in dimension  $n = 30$  to 7 % in dimension  $n = 100$ .

**Remark 1** *For the two toy examples studied so far, projecting  $\hat{\Sigma}^*$  in the Failure-Informed Subspace (FIS) of Uribe et al. (2020) (see the introduction) would outperform our method with  $\hat{\Sigma}_k^*$ , leading to results close to those obtained with  $\Sigma^*$ . However, computing the FIS relies on the knowledge of the gradient of the function  $\varphi$ , which is straightforward to compute in these two toy examples, and it applies to these examples because they are rare-event problems (i.e.,  $\phi$  is of the form  $\phi = \mathbb{I}_{\{\varphi \geq 0\}}$ ). In the next two sections, we present two applications in mathematical finance where the evaluation of the FIS is not feasible since either the function is not differentiable (test case of Section 5.3) or the example is not a rare event simulation problem (test case of Section 5.4).*

### 5.3 Application: large portfolio losses

The next example is a rare event application in finance, taken from Chan and Kroese (2012); Bassamboo et al. (2008). The unknown probability is  $E = \mathbb{P}(L(\mathbf{Z}) > 0)$ , with  $L$  the portfolio loss function defined as:

$$L(\mathbf{z}) = \sum_{j=1}^n \mathbb{I}_{\{z_j \geq 0.5\sqrt{n}\}} - 0.25n.$$

The random inputs  $Z_j$  are dependent variables given by:

$$Z_j = \left( qU + (1 - q^2)^{1/2} \eta_j \right) \mu^{-1/2}$$

with  $U \sim \mathcal{N}(0, 1)$ ,  $\eta_j \sim \mathcal{N}(0, 9)$ ,  $j = 1, \dots, n$ ,  $\mu \sim \text{Gamma}(6, 6)$  are all independent variables, and  $q = 0.25$ . To stay in the scope of standard Gaussian variables, we set  $\eta_j = 3\tilde{\eta}_j$ , for all  $j = 1, \dots, n$  and  $\mu = F_\Gamma^{-1}(F_{\mathcal{N}}(\tilde{\mu}))$  with  $\tilde{\eta}_j, \tilde{\mu}$  independent standard Gaussian variables and  $F_\Gamma, F_{\mathcal{N}}$  the cumulative distribution functions of the Gamma(6, 6) and  $\mathcal{N}(0, 1)$  respectively. Then, setting  $X_1 = U, X_2 = \tilde{\mu}$  and  $(X_3, \dots, X_{n+2}) = \tilde{\eta} \in \mathbb{R}^n$ , we define:

$$\varphi(\mathbf{X}) = \sum_{j=1}^n \mathbb{I}_{\{\psi(U, \tilde{\mu}, \tilde{\eta}_j) \geq 0.5\sqrt{n}\}} - 0.25n \quad (15)$$

with

$$\psi(U, \tilde{\mu}, \tilde{\eta}_j) = \left( qU + 3(1 - q^2)^{1/2} \tilde{\eta}_j \right) \left[ F_\Gamma^{-1}(F_{\mathcal{N}}(\tilde{\mu})) \right]^{-1/2}.$$

Hence the probability of large losses  $\mathbb{P}(L(\mathbf{Z}) > 0)$  can be rewritten as  $\mathbb{P}(\varphi(\mathbf{X}) > 0)$ , with  $\mathbf{X}$  a standard Gaussian random vector of dimension  $n + 2$ . The reference values of this probability  $E$  are reported in Table 4 for dimensions  $n = 30, 70$  and 100. The optimal parameters  $\mathbf{m}^*$  and  $\Sigma^*$  cannot be computed analytically, but they are accurately estimated by Monte Carlo with a large sample. It turns

|                                       |                              | $\Sigma^*$ | $\hat{\Sigma}^*$ | $\hat{\Sigma}_{\mathbf{m}}^* = \hat{\Sigma}_{\mathbf{d}}^*$ | $\hat{\Sigma}_{\mathbf{d}}^*$ | $\hat{\Sigma}_{\mathbf{m}}^*$ |
|---------------------------------------|------------------------------|------------|------------------|---|-------------------------------|-------------------------------|
| $n = 30$<br>$E = 4.29 \cdot 10^{-3}$  | $D'(\Sigma)$                 | 33.37      | 34.64            | 33.63   | 33.71                         | 33.66                         |
|                                       | Relative error (%)           | 0          | 3.8              | 0.78  | 1.0                           | 0.86                          |
|                                       | Mean ( $\times 10^{-3}$ )    | 4.361      | 4.184            | 4.263   | 4.207                         | 4.233                         |
|                                       | Relative bias (%)            | 1.6        | -2.5             | -0.63   | -1.9                          | -1.3                          |
|                                       | Coefficient of variation (%) | 11.3       | 19.9             | 9.7   | 11.1                          | 10.3                          |
| $n = 70$<br>$E = 2.36 \cdot 10^{-3}$  | $D'(\Sigma)$                 | 75.84      | 83.19            | 76.69   | 76.92                         | 76.75                         |
|                                       | Relative error (%)           | 0          | 9.7              | 1.1   | 1.4                           | 1.2                           |
|                                       | Mean ( $\times 10^{-3}$ )    | 2.349      | 3.208            | 2.365   | 2.305                         | 2.359                         |
|                                       | Relative bias (%)            | -0.47      | 36               | 0.21  | -2.3                          | -0.06                         |
|                                       | Coefficient of variation (%) | 7.0        | 350              | 9.2   | 8.2                           | 11.0                          |
| $n = 100$<br>$E = 1.82 \cdot 10^{-3}$ | $D'(\Sigma)$                 | 105.99     | 122.30           | 107.32  | 107.70                        | 107.41                        |
|                                       | Relative error (%)           | 0          | 15.4             | 1.3   | 1.6                           | 1.3                           |
|                                       | Mean ( $\times 10^{-3}$ )    | 1.785      | 1.150            | 1.865   | 1.839                         | 1.814                         |
|                                       | Relative bias (%)            | -1.9       | -37              | 2.5   | 1.0                           | -0.32                         |
|                                       | Coefficient of variation (%) | 10.8       | 73               | 11.3  | 16.5                          | 13.2                          |

Table 4: Numerical comparison of the estimation of  $E$  using the six covariance matrices of Section 3.2 when  $\phi = \mathbb{1}_{\{\varphi \geq 0\}}$  with  $\varphi$  given by (15).

out that  $\mathbf{m}^*$  and the first eigenvector  $\mathbf{d}_1^*$  of  $\Sigma^*$  are numerically indistinguishable and that Algorithm 2 selects  $k = 1$  projection direction, so that we have  $\hat{\Sigma}_{\mathbf{m}}^* = \hat{\Sigma}_{\mathbf{d}}^*$ .

The results of Table 4 show similar trends as for the first toy example of Section 5.1. First, projecting seems indeed a relevant idea, as using  $\hat{\Sigma}_{\mathbf{m}}^* = \hat{\Sigma}_{\mathbf{d}}^*$  greatly improves the situation compared to  $\hat{\Sigma}^*$ . This is particularly salient in dimension  $n = 70$  where  $\hat{\Sigma}^*$  yields a relative bias of 36 % and a coefficient of variation of 350 %, whereas projecting on  $\mathbf{m}^* = \mathbf{d}_1^*$  yields a relative bias of 0.2 % and a coefficient of variation of 9 %. This improvement is still true even when estimations of the projection direction are computed: compared to  $\hat{\Sigma}_{\mathbf{m}}^* = \hat{\Sigma}_{\mathbf{d}}^*$  and in dimension  $n = 100$  for instance,  $\hat{\Sigma}_{\mathbf{d}}^*$  and  $\hat{\Sigma}_{\mathbf{m}}^*$  give smaller relative biases and coefficients of variation between 13 and 16 %, against 11 % for the perfect projection directions. Finally,  $\hat{\Sigma}_{\mathbf{m}}^*$  seems to behave better than  $\hat{\Sigma}_{\mathbf{d}}^*$ : its relative bias is always smaller, and its coefficient of variation also except in dimension  $n = 70$ . As for the first toy example, this can be understood by the fact that  $\hat{\mathbf{m}}^*$  is probably a more accurate estimator of  $\mathbf{m}^* = \mathbf{d}_1^*$  than  $\hat{\mathbf{d}}_1^*$ .

#### 5.4 Application: discretized Asian payoff

Our last numerical experiment is a mathematical finance example coming from Kawai (2018), representing a discrete approximation of a standard Asian payoff under the Black–Scholes model. The goal is to estimate the integral  $E$  with the following function  $\phi$ :

$$\phi : \mathbf{x} = (x_1, \dots, x_n) \mapsto e^{-rT} \left[ \frac{S_0}{n} \sum_{i=1}^n \exp \left( \sum_{k=1}^i \left( r - \frac{\sigma^2}{2} \right) \frac{T}{n} + \sigma \sqrt{\frac{T}{n}} x_k \right) - K \right]_+ \quad (16)$$

where  $[y]_+ = \max(y, 0)$ , for a real number  $y$ . The constants are taken from Kawai (2018):  $S_0 = 50$ ,  $r = 0.05$ ,  $T = 0.5$ ,  $\sigma = 0.1$ ,  $K = 55$ , where they test the function for dimension  $n = 16$ . In our contribution, we also test this example in dimension 40 and 100. Concerning  $\mathbf{m}^*$  and the  $\mathbf{d}_i^*$ 's, the situation is the same as in the previous example: they are not available analytically but can be estimated numerically by Monte Carlo with a large simulation budget. And again, it turns out that  $\mathbf{m}^*$  and the first eigenvector  $\mathbf{d}_1^*$  of  $\Sigma^*$  are numerically indistinguishable and that Algorithm 2 selects  $k = 1$  projection direction, so that we have  $\hat{\Sigma}_{\mathbf{m}}^* = \hat{\Sigma}_{\mathbf{d}}^*$ . Although for the first toy example of Section 5.1 it is clear why we should have  $\mathbf{m}^* = \mathbf{d}_1^*$ , we find it striking that in the two numerical examples coming from real-world applications we also have this. We will elaborate on this in the conclusion.

|                                       |                              | $\Sigma^*$ | $\hat{\Sigma}^*$ | $\hat{\Sigma}_{\mathbf{m}}^* = \hat{\Sigma}_{\mathbf{d}}^*$ | $\hat{\Sigma}_{\mathbf{d}}^*$ | $\hat{\Sigma}_{\mathbf{m}}^*$ |
|---------------------------------------|------------------------------|------------|------------------|---|-------------------------------|-------------------------------|
| $n = 16$<br>$E = 2.45 \cdot 10^{-2}$  | $D'(\Sigma)$                 | 14.33      | 15.15            | 14.38   | 14.51                         | 14.40                         |
|                                       | Relative error (%)           | 0          | 5.7              | 0.33  | 1.2                           | 0.47                          |
|                                       | Mean ( $\times 10^{-2}$ )    | 2.449      | 2.463            | 2.448   | 2.457                         | 2.455                         |
|                                       | Relative bias (%)            | -0.05      | 0.52             | -0.07   | 0.29                          | 0.20                          |
|                                       | Coefficient of variation (%) | 1.7        | 6.7              | 1.6   | 2.2                           | 1.7                           |
| $n = 40$<br>$E = 2.04 \cdot 10^{-2}$  | $D'(\Sigma)$                 | 38.07      | 43.45            | 38.25   | 38.64                         | 38.30                         |
|                                       | Relative error (%)           | 0          | 14.1             | 0.47  | 1.5                           | 0.60                          |
|                                       | Mean ( $\times 10^{-2}$ )    | 2.026      | 1.968            | 2.027   | 2.007                         | 2.024                         |
|                                       | Relative bias (%)            | -0.71      | -3.5             | -0.66   | -1.6                          | -0.78                         |
|                                       | Coefficient of variation (%) | 1.7        | 35               | 3.2   | 3.9                           | 2.1                           |
| $n = 100$<br>$E = 1.87 \cdot 10^{-2}$ | $D'(\Sigma)$                 | 97.13      | 137.86           | 98.05   | 99.56                         | 98.17                         |
|                                       | Relative error (%)           | 0          | 42               | 0.94  | 2.5                           | 1.1                           |
|                                       | Mean ( $\times 10^{-2}$ )    | 1.874      | 0.114            | 1.874   | 1.788                         | 1.856                         |
|                                       | Relative bias (%)            | 0.20       | -94              | 0.23  | -4.4                          | -0.74                         |
|                                       | Coefficient of variation (%) | 3.1        | 94               | 2.6   | 9.1                           | 2.5                           |

Table 5: Numerical comparison of the estimation of  $E$  using the six covariance matrices of Section 3.2 when  $\phi$  is given by (16).

The results of this example are given in Table 5. The insight gained in the previous examples is confirmed. Projecting on  $\mathbf{m}^* = \mathbf{d}_1^*$  in dimension  $n = 100$  for instance reduces (compared to  $\hat{\Sigma}^*$ ) the relative bias from  $-94\%$  to  $0.2\%$  and the coefficient of variation from  $94\%$  to  $2.6\%$ . Moreover, this improvement goes through even when projection directions are estimated, with again  $\hat{\Sigma}_{\mathbf{m}}^*$  behaving better than  $\hat{\Sigma}_{\mathbf{d}}^*$ .

## 6 Conclusion

The goal of this paper is to assess the efficiency of projection methods in order to overcome the curse of dimensionality for importance sampling. Based on a new theoretical result (Theorem 1), we propose to project on the subspace spanned by the eigenvectors  $\mathbf{d}_i^*$ 's corresponding to the smallest (in  $\ell$ -order) eigenvalues of the optimal covariance matrix  $\Sigma^*$ . Our numerical results show that if the  $\mathbf{d}_i^*$ 's were perfectly known, then projecting on them (column  $\hat{\Sigma}_{\mathbf{d}}^*$  in Tables 2–5) would greatly improve the final estimation compared to using the empirical estimation of the covariance matrix (column  $\hat{\Sigma}^*$ ) and actually lead to results which are comparable to those obtained with the optimal covariance matrix (column  $\Sigma^*$ ). Moreover, we show that this improvement goes through when one estimates the  $\mathbf{d}_i^*$ 's (column  $\hat{\Sigma}_{\mathbf{d}}^*$ ) by computing the eigenpairs of  $\hat{\Sigma}^*$ : indeed, using  $\hat{\Sigma}_{\mathbf{d}}^*$  as covariance matrix instead of  $\hat{\Sigma}^*$  gives results which remain accurate up to the dimension  $n = 100$  considered in the present paper.

Moreover, we compare the directions  $\mathbf{d}_i^*$ 's, which are justified by Theorem 1, with the algorithm proposed in El Masri et al. (2020) which amounts to projecting on  $\mathbf{m}^*$  (column  $\hat{\Sigma}_{\mathbf{m}}^*$  when  $\mathbf{m}^*$  is assumed to be known, or column  $\hat{\Sigma}_{\mathbf{m}}^*$  when one uses the estimation  $\hat{\mathbf{m}}^*$  of  $\mathbf{m}^*$ ). Our findings in this case are quite surprising: on three out of the four numerical examples considered, it turns out that  $\mathbf{m}^* = \mathbf{d}_1^*$  (at least, they are numerically indistinguishable) and Algorithm 2 selects one projection direction so that  $\hat{\Sigma}_{\mathbf{m}}^* = \hat{\Sigma}_{\mathbf{d}}^*$ . Although for the first example of Section 5.1 the relation  $\mathbf{m}^* = \mathbf{d}_1^*$  is easy to get thanks to the high symmetry of the problem at hand, for the concrete applications of Sections 5.3 and 5.4 this is more surprising. The second toy example of Section 5.2 was precisely built in order to break the relation between  $\mathbf{m}^*$  and  $\mathbf{d}_1^*$ , and in this case,  $\hat{\Sigma}_{\mathbf{d}}^*$  clearly outperforms  $\hat{\Sigma}_{\mathbf{m}}^*$ . It would be interesting to delve deeper into the relation between  $\mathbf{m}^*$  and the eigenvectors of  $\Sigma^*$ , and try and understand when estimating the  $\mathbf{d}_i^*$ 's instead of the simpler  $\mathbf{m}^*$  is indeed worthwhile.

All in all, these theoretical and numerical results show that the  $\mathbf{d}_i^*$ 's of Theorem 1 are good directions in which to estimate variance terms. As explained in Section 3.2, we chose the simplest possible



numerical framework in order to assess this. With the insight gained, we see several ways to extend our results. Two in particular stand out:

1. study different ways of estimating the eigenpairs  $(\lambda_i^*, \mathbf{d}_i^*)$ ;
2. incorporate this method in adaptive importance sampling schemes, in particular the cross-entropy method.

For the first point, remember that we made the choice to estimate the eigenpairs of  $\Sigma^*$  by computing the eigenpairs of  $\hat{\Sigma}^*$ . Moreover, in the numerical examples of Sections 5.1, 5.3 and 5.4 where  $\mathbf{m}^* = \mathbf{d}_1^*$ , we saw that  $\hat{\Sigma}_{\hat{\mathbf{m}}}^*$  performed better than  $\hat{\Sigma}_{\hat{\mathbf{d}}}^*$  and we conjecture that this is because  $\hat{\mathbf{m}}$  is a better estimator of  $\mathbf{m}^* = \mathbf{d}_1^*$  than  $\hat{\mathbf{d}}$ . This suggests that improving the estimation of the  $\mathbf{d}_i^*$ 's can indeed improve the final estimation of  $E$ . Possible ways to do so consist in adapting existing results on the estimation of covariance matrices (for instance Ledoit and Wolf (2004)) or even directly results on the estimation of eigenvalues of covariance matrices such as in Mestre (2008b,a); Benaych-Georges and Nadakuditi (2011); Nadakuditi and Edelman (2008), which we plan to do in future work. Moreover, it would be interesting to relax the assumption that one can sample from  $g^*$  in order to estimate  $\hat{\Sigma}^*$ . For the second point, we plan to investigate how the idea of the present paper can improve the efficiency of adaptive importance sampling schemes in high dimension. In this case, there is an additional difficulty, namely the introduction of likelihood ratios can lead to the problem of weight degeneracy which is another reason why performance of such schemes degrades in high dimension (See Bengtsson et al. (2008)).

We note finally that it would be interesting to consider multimodal failure functions  $\phi$ . Indeed, with unimodal functions, the light tail of the Gaussian random variable implies that the conditional variance decreases which explains why, in all our numerical examples, the smallest eigenvalues ranked in  $\ell$ -order are simply the smallest eigenvalues. However, for multimodal failure functions, we may expect the conditional variance to increase and that the smallest eigenvalues ranked in  $\ell$ -order are actually the largest ones. For multimodal problems, one may want to consider different parametric families of auxiliary densities, and so it would be interesting to see whether Theorem 1 can be extended to more general cases.

## References

- Agapiou S, Papaspiliopoulos O, Sanz-Alonso D, Stuart AM (2017) Importance Sampling : Intrinsic Dimension and Computational Cost. *Statistical Science*, Volume 32, p405-431
- Ashurbekova K, Usseglio-Carleve A, Forbes F, Achard S (2020) Optimal shrinkage for robust covariance matrix estimators in a small sample size setting. hal-02378034v2
- Au S, Beck J (2003) Important sampling in high dimensions. *Structural Safety* 25(2):139–163, DOI 10.1016/S0167-4730(02)00047-4
- Bassamboo A, Juneja S, Zeevi A (2008) Portfolio Credit Risk with Extremal Dependence: Asymptotic Analysis and Efficient Simulation. *Operations Research* 56(3):593–606, DOI 10.1287/opre.1080.0513
- Benaych-Georges F, Nadakuditi RR (2011) The eigenvalues and eigenvectors of finite, low rank perturbations of large random matrices. *Advances in Mathematics* 227(1):494–521, DOI <https://doi.org/10.1016/j.aim.2011.02.007>, URL <https://www.sciencedirect.com/science/article/pii/S0001870811000570>
- Bengtsson T, Bickel P, Li B (2008) Curse-of-dimensionality revisited: Collapse of the particle filter in very large scale systems. In: *Institute of Mathematical Statistics Collections*, Institute of Mathematical Statistics, Beachwood, Ohio, USA, pp 316–334, DOI 10.1214/193940307000000518
- Bucklew J (2013) *Introduction to rare event simulation*. Springer Science & Business Media
- Bugallo MF, Elvira V, Martino L, Luengo D, Miguez J, Djuric PM (2017) Adaptive Importance Sampling: The past, the present, and the future. *IEEE Signal Processing Magazine* 34(4):60–79, DOI 10.1109/MSP.2017.2699226

- Cappé O, Douc R, Guillin A, Marin JM, Robert CP (2008) Adaptive importance sampling in general mixture classes. *Statistics and Computing* 18(4):447–459, DOI 10.1007/s11222-008-9059-x
- Chan JCC, Kroese DP (2012) Improved cross-entropy method for estimation. *Statistics and Computing* 22(5):1031–1040, DOI 10.1007/s11222-011-9275-7
- Chatterjee S, Diaconis P (2018) The sample size required in importance sampling. *Ann Appl Probab* 28(2):1099–1135
- Cornuet JM, Marin JM, Mira A, Robert CP (2012) Adaptive Multiple Importance Sampling: *Adaptive multiple importance sampling*. *Scandinavian Journal of Statistics* 39(4):798–812, DOI 10.1111/j.1467-9469.2011.00756.x
- El-Laham Y, Elvira V, Bugallo M (2019) Recursive shrinkage covariance learning in adaptive importance sampling. In: 2019 IEEE 8th International Workshop on Computational Advances in Multi-Sensor Adaptive Processing (CAMSAP), IEEE, pp 624–628
- El Masri M, Morio J, Simatos F (2020) Improvement of the cross-entropy method in high dimension through a one-dimensional projection without gradient estimation. arXiv:201211241 [stat] [2012.11241](#)
- Grace AW, Kroese DP, Sandmann W (2014) Automated State-Dependent Importance Sampling for Markov Jump Processes via Sampling from the Zero-Variance Distribution. *Journal of Applied Probability* 51(3):741–755, DOI 10.1239/jap/1409932671
- Hohenbichler M, Rackwitz R (1981) Non-Normal Dependent Vectors in Structural Safety. *Journal of the Engineering Mechanics Division* 107(6):1227–1238, DOI 10.1061/JMCEA3.0002777
- Kawai R (2018) Optimizing Adaptive Importance Sampling by Stochastic Approximation. *SIAM Journal on Scientific Computing* 40(4):A2774–A2800, DOI 10.1137/18M1173472
- Ledoit O, Wolf M (2004) A well-conditioned estimator for large-dimensional covariance matrices. *Journal of Multivariate Analysis* 88(2):365–411, DOI 10.1016/S0047-259X(03)00096-4
- Liu PL, Der Kiureghian A (1986) Multivariate distribution models with prescribed marginals and covariances. *Probabilistic Engineering Mechanics* 1(2):105–112, DOI 10.1016/0266-8920(86)90033-0
- Mestre X (2008a) Improved Estimation of Eigenvalues and Eigenvectors of Covariance Matrices Using Their Sample Estimates. *IEEE Transactions on Information Theory* 54(11):5113–5129, DOI 10.1109/TIT.2008.929938
- Mestre X (2008b) On the Asymptotic Behavior of the Sample Estimates of Eigenvalues and Eigenvectors of Covariance Matrices. *IEEE Transactions on Signal Processing* 56(11):5353–5368, DOI 10.1109/TSP.2008.929662
- Nadakuditi RR, Edelman A (2008) Sample eigenvalue based detection of high-dimensional signals in white noise using relatively few samples. *IEEE Transactions on Signal Processing* 56(7):2625–2638, DOI 10.1109/TSP.2008.917356
- Owen A, Zhou Y (2000) Safe and Effective Importance Sampling. *Journal of the American Statistical Association* 95(449):135–143, DOI 10.1080/01621459.2000.10473909
- Papaioannou I, Geyer S, Straub D (2019) Improved cross entropy-based importance sampling with a flexible mixture model. *Reliability Engineering & System Safety* 191:106564, DOI 10.1016/j.res.2019.106564
- Rubinstein RY, Kroese DP (2011) *The Cross-Entropy Method: A Unified Approach to Combinatorial Optimization, Monte-Carlo Simulation and Machine Learning*. Springer, New York; London
- Rubinstein RY, Kroese DP (2017) *Simulation and the Monte Carlo Method*, third edition edn. Wiley Series in Probability and Statistics, Wiley, Hoboken, New Jersey
- Uribe F, Papaioannou I, Marzouk YM, Straub D (2020) Cross-entropy-based importance sampling with failure-informed dimension reduction for rare event simulation. arXiv:200605496 [stat] [2006.05496](#)